

Dept. of Cranio-Maxillofacial and Oral Surgery
Oral Biotechnology & Bioengineering

**3D-printed bone substitutes
 with triply periodic minimal surface
 microarchitectures**

Franz E. Weber
 Prof. Dr. rer. nat. habil.



Universität Zürich

USZ Universitäts
 Spital Zürich

Natural bone microarchitecture is gothic style

Microstructure of the Distal Radius and Its Relevance to Distal Radius Fractures

Gregory Ian Bain, MBBS, FRACS, FA, PhD¹ Simon Bruce Murdoch MacLennan, MBChB, FRCS(Ed), PGDipCE² Tom McNaughton, MBChB, BSc² Ruth Williams³

¹Department of Orthopaedic Surgery, Flinders University, Adelaide, South Australia, Australia
²Faculty of Medicine, Faculty of Medicine and Health, University of South Wales, United Kingdom
³Adelaide Microscopy, Waikell School, The University of Adelaide, Adelaide, South Australia, Australia

Address for correspondence: Simon Bruce Murdoch MacLennan, MBChB, FRCS(Ed), Department of Orthopaedic Surgery, Flinders Medical Centre, Bedford Park, SA 5042, Adelaide, Australia (Email: simonmac@flinders.edu.au)

© 2016 Wiley Periodicals, Inc.

Load orchestrates microarchitecture.

Trabecular microarchitecture takes up the load directly and is constantly adjusted to actual loads during bone turnover (Wolff's law)

There is no evolutionary pressure on the microarchitecture of bone for optimization of osteoconductivity.

No need for biomimetics, since osteoconduction is an artificial although clinically highly relevant phenomenon.

Biomimetic or technomimetic microarchitecture

Trabecular bone (rod-like structure) Biocomposite PLA/β-TCP composite processed by a supercritical CO₂ foaming methodology

bone is a lightweight, load-driven, gothic style 3D-structure aiming towards high strength

Biomimetic look alike

“technomimetics”

Adaptive Density Minimal Surface (ADMS) algorithm

lightweight 3D-structure high strength/low material in aerospace, aviation and EV

Strength of implant is optimized for a single location all locations

trabecular bone ADMS microarchitecture

Osteoconduction

lightweight microarchitectures

lattice
strait

ADMS/TPMS
curvy

Strait and curvy microarchitectures can be highly osteoconductive

Maevskaia et al. „Weber FE 3D Printing & Additive Manufacturing (2022)

Triply periodic minimal surface lightweight microarchitectures (TPMS)

Mathematical problem posed by the "königliche Akademie der Wissenschaften zu Berlin 1865":
Minimal surface formed between four points located each on one of the four sides of a tetrahedron.

Ueber die Minimalfläche, deren Begrenzung als ein von vier Kanten eines regulären Tetraeders gebildetes räumliches Viereck gegeben ist. (Im April 1865 von Herrn Kummer der Königl. Akademie der Wissenschaften zu Berlin mitgetheilt. Monatsberichte der Königl. Akademie der Wissenschaften zu Berlin, Jahrgang 1865, Seite 149–153.)

Schwartz 1890

P primitive and D diamond

Triply periodic minimal surface lightweight microarchitectures (TPMS)

Mathematical problem posed by the "königliche Akademie der Wissenschaften zu Berlin 1865":
Minimal surface formed between four points located each on one of the four sides of a tetrahedron.

Schwartz 1890

P primitive and D diamond

Schoen 1970

G gyroid


Triply periodic minimal surface microarchitectures (TPMS) as primitive, diamond and gyroid are:

- **lightweight** minimal surface at a given thickness of the material).
- **omni-isotropic**, i.e. non-self-intersecting, periodic surface structures in three principal directions
- Zero mean curvature, leading to a **uniform stress** distribution under load and **high strength**

TPMS are high strength lightweight microarchitectures

Natural TPMS-lightweight microarchitectures

Gyroid

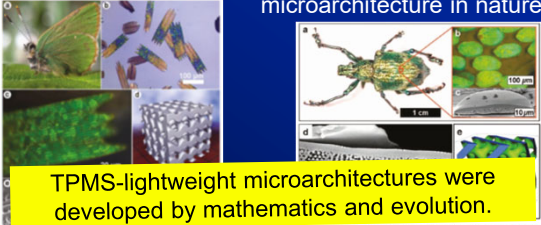


36 gyroids were designed by Nintendo to be found in Animal Crossing ©

Natural TPMS-lightweight microarchitectures

Gyroid in butterfly wings Diamond in exoskeleton of a beetle

microarchitecture in nature



TPMS-lightweight microarchitectures were developed by mathematics and evolution.

Figure 4. a) Photograph of C. oak. b) Optical microscope image of both colored and brown flower scales. c) High-resolution SEM image of an individual scale showing that the photonic band gap arises from many individual SC domains. d) Computer-generated SC model. e) SEM image of a flower scale showing the diamond-like surface with SC domains in different orientations. Reproduced under the terms of the CC-BY license (Creative Commons 2015). The authors: R. W. Corkery, E. C. Tyrone, *Interface Focus* 2017, 7, 20160184. *Colophrys rubi* (Linnaeus, 1758) Grüne Ziefelfalter

Figure 6. a) Photograph of the weevil *I. scapularis*. b) Optical microscope image of individual scales attached to the exoskeleton. c) Angular and white light transmission. d) Cross-sectional SEM image of a single scale. e) Detailed cross-sectional SEM image of a region of a scale. f) Schematic drawing of the SC structure. Reproduced with permission (Copyright 2004, American Physical Society). J. W. Galusha, L. R. Ritchey, J. S. Gardner, J. N. Cha, M. H. Bart, *Phys. Rev. E* 2008, 77, 055904. *Lamprocyphus rugosus*, Rosenfelder

Lu Han* and Shunai Che, *Adv. Mater.* 2018, 30, 1705708

TPMS-lightweight microarchitectures

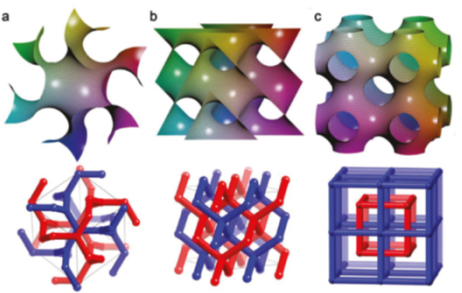


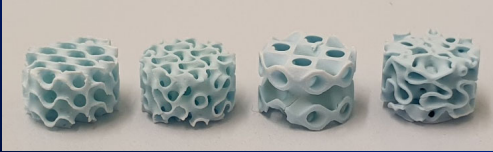
Figure 1. Schematic drawings and skeletal graphs of TPMSs: a) G surface, b) D surface, and c) P surface.

Lu Han* and Shunai Che, *Adv. Mater.* 2018, 30, 1705708



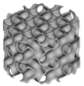
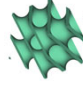
TPMS-lightweight microarchitectures

Additive manufacturing enables the production of D-, G-, P- triply periodic minimal surface microarchitectures and ADMS adaptive density minimal surface (only periodic)



D- diamond G-gyroid P-primitive ADMS

How to create TPMS designs

Cell unit	Final shape	TPMS equation
		Gyroid: $\sin(x) \cos(y) + \sin(y) \cos(z) + \sin(z) \cos(x)$
		Diamond: $\sin(x) \sin(y) \sin(z) + \sin(x) \cos(y) \cos(z) + \cos(x) \sin(y) \cos(z) + \cos(x) \cos(y) \sin(z)$
		Primitive: $\cos(x) + \cos(y) + \cos(z)$



Gyroid:
 $\sin(x) \cos(y) + \sin(y) \cos(z) + \sin(z) \cos(x)$



Diamond:
 $\sin(x) \sin(y) \sin(z) + \sin(x) \cos(y) \cos(z) + \cos(x) \sin(y) \cos(z) + \cos(x) \cos(y) \sin(z)$

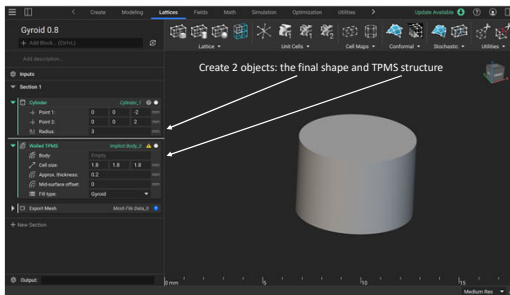


Primitive:
 $\cos(x) + \cos(y) + \cos(z)$

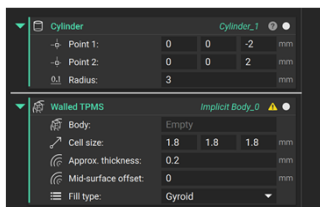
The order of actions

- 1 Create a structure with nTopology
- 2 Check parameters with Fusion 360
- 3 Prepare the file for printing with the slicer
- 4 Print the scaffolds
- 5 Sinter at the desired temperature

nTop

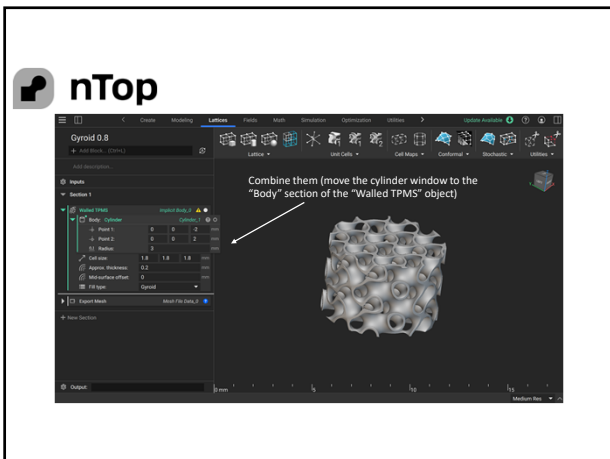


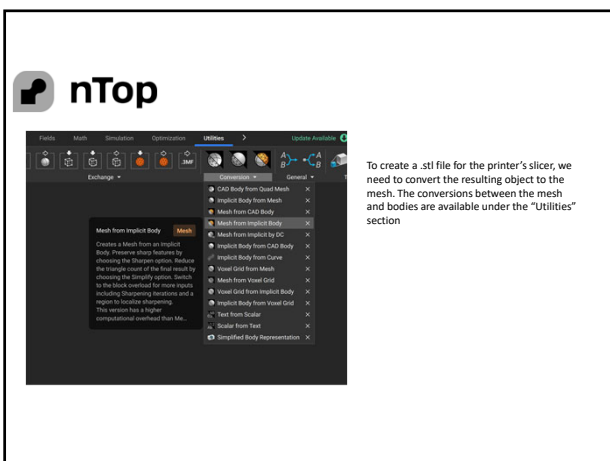
nTop

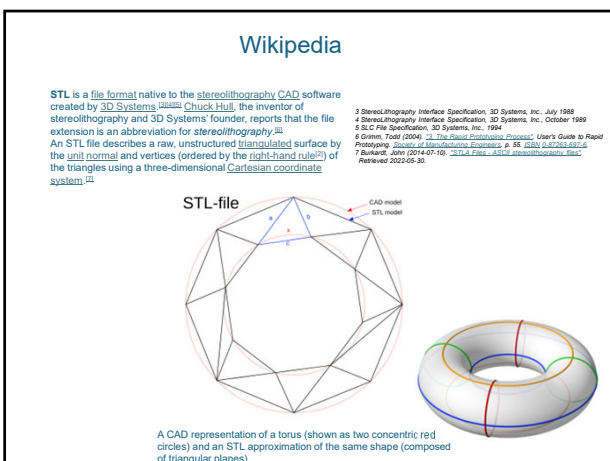


The shape (a cylinder in our case) can be determined by the points in space (x, y, and z axis) and its radius

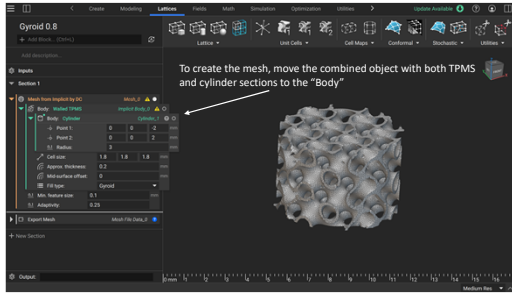
There are preinstalled TPMS types (Gyroid, Diamond, Primitive, and some others) that can be chosen; the size of the cell unit as well as the thickness of the walls can be changed



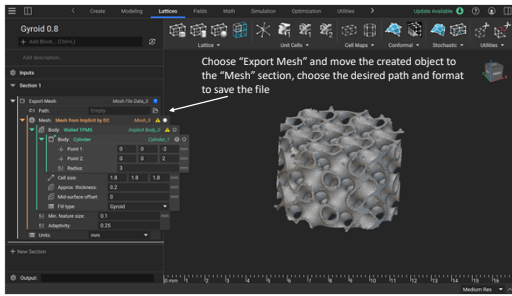




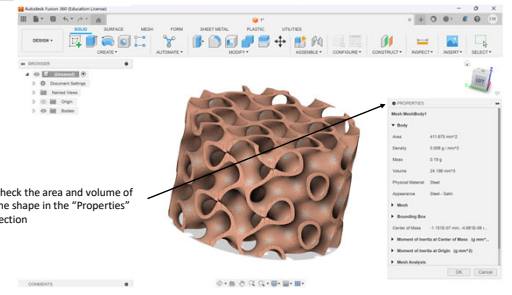
nTop

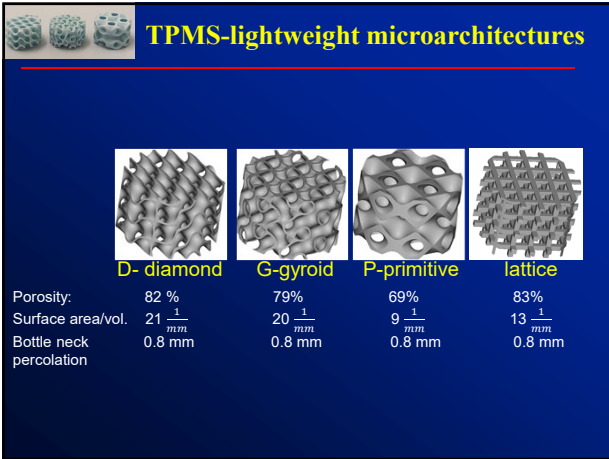


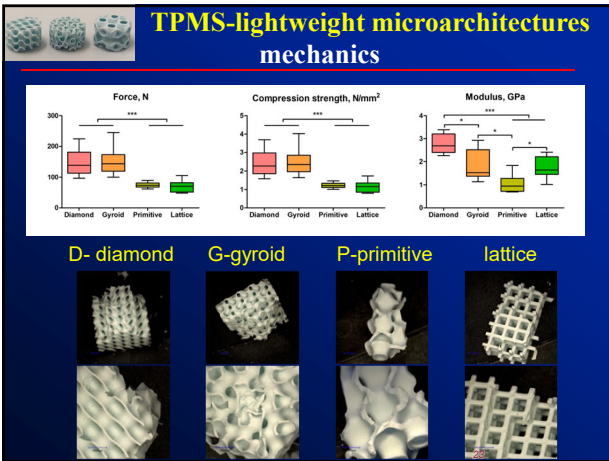
nTop

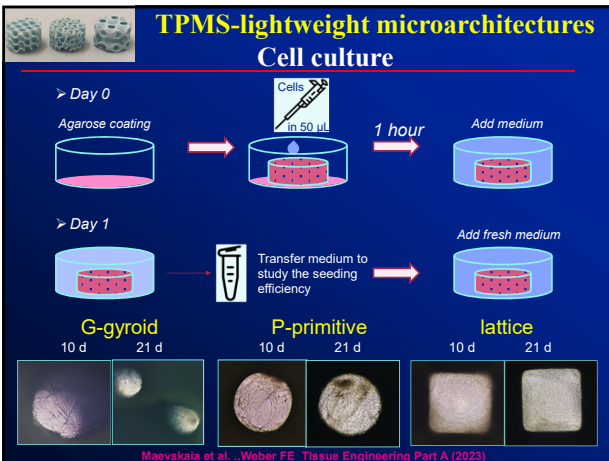


AUTODESK Fusion 360

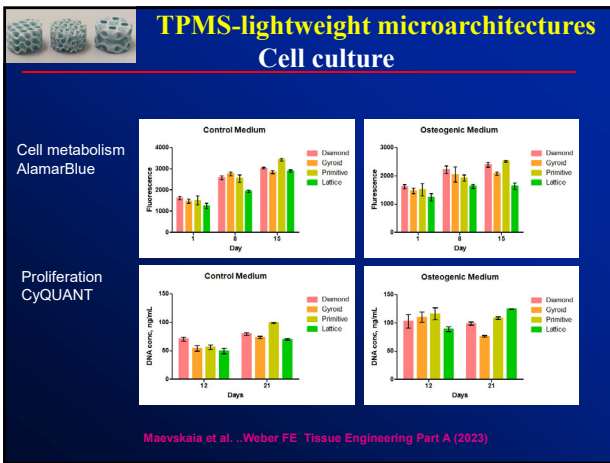


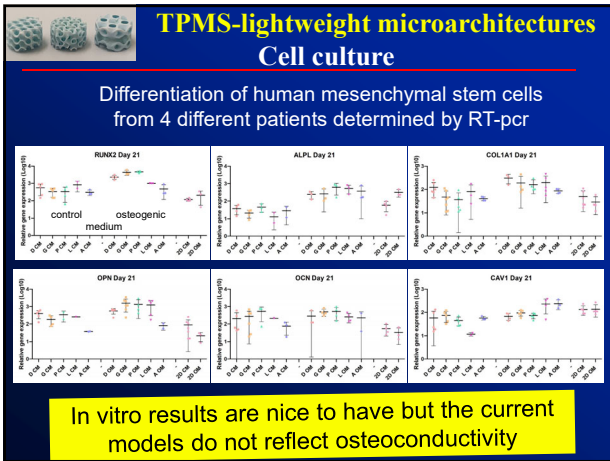


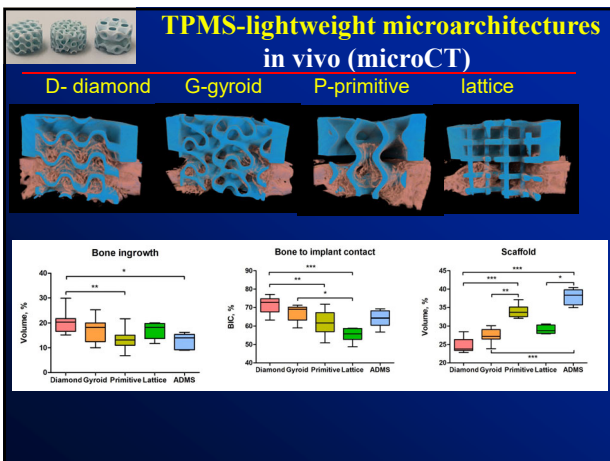


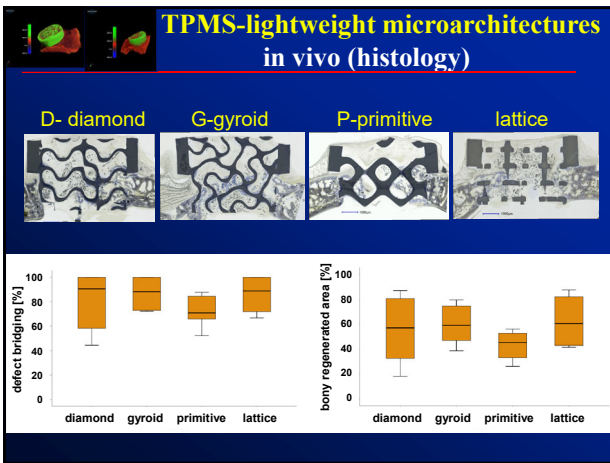


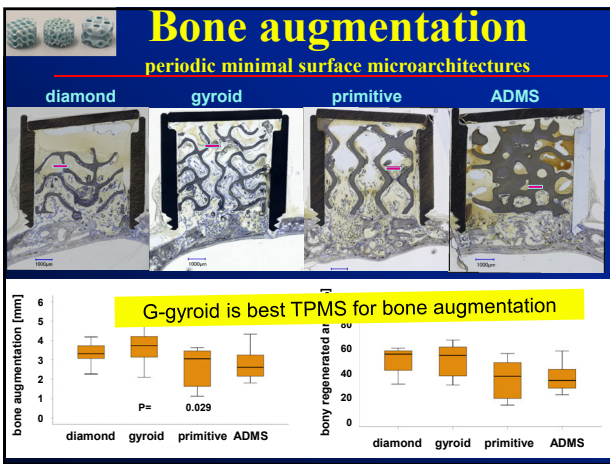
Maevskaia et al. ...Weber FE Tissue Engineering Part A (2023)

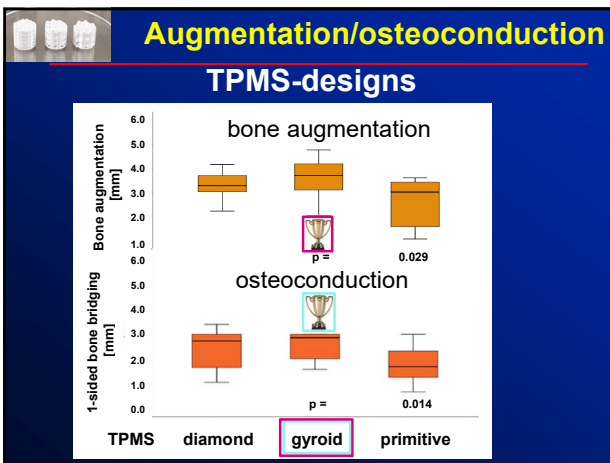












Introduction Design BMSCs exosomes OBS exosomes Conclusion

Exosomes

- ✓
 - Low immunogenicity and toxicity
 - Biocompatibility
 - Stability
 - Less strict storage condition
- ✗
 - Long waiting times due to cell expansion
 - Large doses
- ?
- Cargo
- Optimal source
- Dosage
- Duration of treatment

31

The goal is the development of ceramic-based bone grafts functionalized with exosomes

Strategies:

1. Scaffold design
2. Functionalization of scaffolds

32

Functionalization of scaffolds with BMSCs exosomes

- Characterization of cells and exosomes
- Interaction of cells with exosomes
- Interaction of cells with exosomes within scaffolds
- Implantation of scaffolds with exosomes

Introduction | Design | **BMSCs exosomes** | OBs exosomes | Conclusion

Extraction of BMSCs and exosomes

The process starts with a rabbit, from which bone marrow is extracted. This is used to isolate BMSCs. The BMSCs are then cultured in exosome-free FBS for 24 hours. The medium is then mixed with PBS and centrifuged at 10000 x g for 1 hour. Finally, the medium is treated with an exosome isolation reagent to extract the exosomes.

34

Introduction | Design | **BMSCs exosomes** | OBs exosomes | Conclusion

Nanoparticle tracking analysis

Amount of exosomes (30-200 nm): $4.03 \cdot 10^8 \pm 5.37 \cdot 10^7$ particles/scaffold

Release, %

Release, %

Days

HA TCP

➤ Slower release with Gyroid and TCP scaffolds

Maevskaia E et al. Int. J. Mol. Sci. 2024

35

Introduction | Design | **BMSCs exosomes** | OBs exosomes | Conclusion

Proteomics analysis

Functional Genomics Center Zurich by LC-MS/MS DIA method

Bioinformatics assay: GENOMATOLOGY, UniProt, STRING

Comparison with ExoCarta website

BMSCs exosomes: 461
ExoCarta: 40
Overlap: 62

➤ Proteins were extracted from exosomes

Biological Processes

➤ Proteins associated with bone and cartilage development, angiogenesis

Maevskaia E et al. Int. J. Mol. Sci. 2024

36

Introduction | Design | **BMSCs exosomes** | OBs exosomes | Conclusion

Migration of BMSCs

Testing conditions:
 ➤ Negative control: starvation medium
 ➤ Positive control: 20% FBS or exosome-free FBS

200 µL of starvation medium + cells
 500 µL of medium with exosomes or 20% FBS

24 hours

Upper part
 Lower part

Maevskaia E et al. Int. J. Mol. Sci. 2024 37

Introduction | Design | **BMSCs exosomes** | OBs exosomes | Conclusion

Migration of BMSCs

200 µL of starvation medium + cells

24 hours

500 µL of medium with exosomes or 20% FBS

Maevskaia E et al. Int. J. Mol. Sci. 2024 38

Introduction | Design | **BMSCs exosomes** | OBs exosomes | Conclusion

Migration of BMSCs

Starvation medium | 1x10⁸ exosomes
 2x10⁸ exosomes | 4x10⁸ exosomes

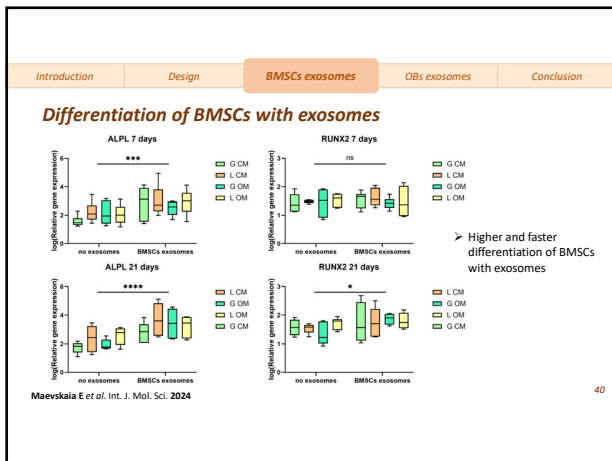
Migration
 $p = 0.002$

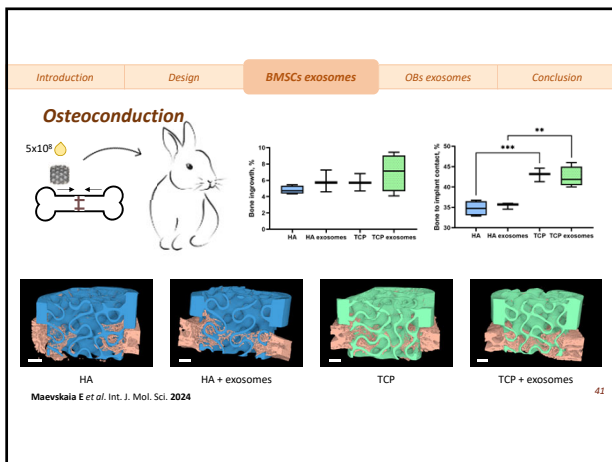
Cells/area

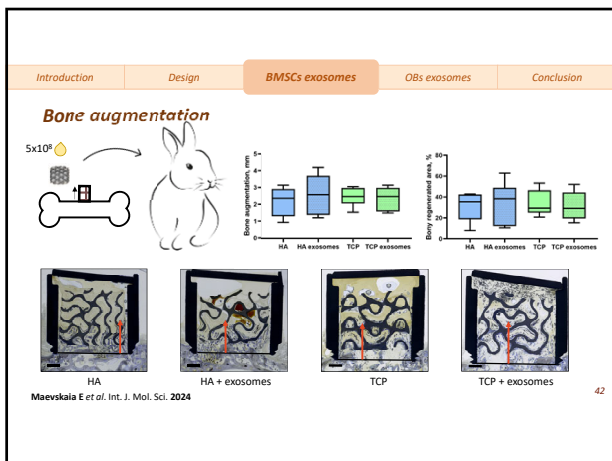
Amount of exosomes

➤ Addition of exosomes stimulates cells' migration

Maevskaia E et al. Int. J. Mol. Sci. 2024 39







Introduction	Design	BMSCs exosomes	OBS exosomes	Conclusion
--------------	--------	-----------------------	--------------	------------

Conclusion of the second part

- Slower release of exosomes from TCP and Gyroid scaffolds
- Proteins associated with bone development
- Earlier differentiation of cells cultured with exosomes
- Higher bone to implant contact with TCP scaffolds

Maevskaia E, Guerrero J, Ghayor C, et al. Functionalization of Ceramic Scaffolds with Exosomes from Bone Marrow Mesenchymal Stromal Cells for Bone Tissue Engineering. International Journal of Molecular Sciences 2024. 25(7):3826. <https://doi.org/10.3390/ijms25073826>

43

Microarchitecture orchestrates osteoconduction and bone augmentation

Reduction of filament dimension and distance from 1.25 to 0.50 mm induces early stage differentiation and angiogenesis and translates into osteoconductivity

The choice of the microarchitecture matters for osteoconduction and bone augmentation. Gyroid and diamond appear superior.

Strait and curvy microarchitectures can be highly osteoconductive. No need for biomimetics

Gyroid and diamond combine good osteoconductivity and high mechanics of scaffold at minimal surface
=minimal material and minimal problems with degradation

Principles of bone tissue engineering

Biomaterial Scaffold

Microarchitecture is a key factor for optimized osteoconduction and bone augmentation

can be realized and studied by additive manufacturing

Additive manufacturing will be center stage for personalized bone substitutes in
Cranio-maxillofacial Surgery
Orthopedics
Dentistry

Thank you

Center of Dental Medicine
Cranio-Maxillofacial and Oral Surgery
Oral Biotechnology & Bioengineering
Zurich, Switzerland
Chafik Ghayor
Indranil Bhattacharya
Ekaterina Maevskaia
Julien Guerrero
Ana Perez

Center of Dental Medicine
Clinic of Reconstructive
Dentistry
Mutlu Ozcan

University of Applied Sciences
Northwestern Switzerland
Muttenz, Switzerland
Michael de Wild
Daniel Seiler

University Hospital
Zurich, Switzerland
BZL
Flora Nicholls

Spharone
Zurich, Switzerland
Christian Waldvogel
Daniel Salamon
Niklaus Arn

Lithoz
Vienna, Austria
Johannes Homa
Martin Schwentenwein

for your attention